

THE DEOS AUTOMATION AND ROBOTICS PAYLOAD
ESA/ESTEC, NOORDWIJK, THE NETHERLANDS / 12 – 14 APRIL 2011

P. Rank⁽¹⁾, Q. Mühlbauer⁽¹⁾, W. Naumann⁽²⁾, K. Landzettel⁽³⁾

⁽¹⁾Kayser-Threde, Munich, Germany, Email: {peter.rank, quirin.muehlbauer}@kayser-threde.com

⁽²⁾SpaceTech GmbH, Immenstaad, Germany, Email: walter.naumann@spacetechnology.com

⁽³⁾Institute of Robotics and Mechatronics, DLR-RM, Oberpfaffenhofen, Germany, Email: klaus.landzettel@dlr.de

ABSTRACT

Challenging on-orbit servicing techniques and procedures are required to demonstrate the capturing of an uncooperative tumbling target satellite with a robotic arm during the “Deutsche Orbitale Servicing Mission” (DEOS). In the DEOS mission [1] capturing and other on-orbit servicing experiments based on robotic manipulation will be conducted under a series of diverse conditions. Application of specific rendezvous and approach techniques allows the chaser satellite (Servicer) to get close enough to the target (Client) whilst remaining within safe range, and maintain the position with sufficient accuracy and stability during the robotic operation. This paper presents the robotic functions, the robot control technique, on-board support hardware for berthing of the Client satellite, and the software support by image processing.

1. INTRODUCTION

DEOS Mission objectives are sub-divided in primary and secondary DEOS mission goals. The primary mission goals comprise capturing of a tumbling and non-cooperative satellite by a manipulator and controlled re-entry of the rigidly coupled satellites within a given re-entry corridor. Secondary mission goals comprise demonstration of the capturing procedure applying different methods with a free floating servicer in tele-presence operation and in autonomous operation, demonstration of the on-orbit servicing capabilities such as in-orbit replacement of a component and capturing of an attitude controlled satellite. These tasks will be conducted under different environmental conditions. For all these tasks the Automation and Robotics (A&R) payload plays a central role. Most A&R payload elements involved in the execution of related tasks will be accommodated on the servicer satellite. A separate Rendezvous and Docking (RvD) payload on the Servicer Satellite is responsible for target acquisition, for flight manoeuvres (e.g. controlled approach to the client satellite), for maintaining a constant distance during robotic demonstrations, and for conducting docking manoeuvres.

The Servicer and the Client satellite will be launched in a stack configuration and will be injected into a near polar orbit with an initial orbit height < 600km which in

the course of the 1 year mission will be stepwise decreased to 450km and 400km. Changing the altitude leads to decreasing contact times and thus also to an increasing complexity of robotic operation tasks, especially during tele-operation sequences. Designs of the A&R payload and the Payload Control System (PCS) on ground shall demonstrate compatibility with this constraint. Another major constraint is the short contact time - when both satellites are within the Weilheim visibility range, not more than 8 minutes are available for the execution of the tasks including sufficient margin for potential contingencies. Even if OOS experiments are on the list of secondary mission goals, they will be performed before the irreversible separation of the satellites, as they represent a lower mission risk. Further constraints defined by the overall mission and system design approach are given in [1].

The remainder of this paper is organized as follows: Section 2 introduces the basic functions of the A&R Payload, followed by a detailed description of the major components on the Servicer and on Ground. The paper concludes with a summary in Section 5.

2. FUNCTIONS OF THE AUTOMATION AND ROBOTICS PAYLOAD

2.1. Berthing of the Client Satellite

The most exceptional A&R payload task on DEOS is the capturing of a tumbling Client satellite followed by its stabilization and finally by transfer of the Client to the berthing position. The capturing sequence is illustrated in Fig. 1. For simulation of both a cooperative and a non-cooperative target, the client satellite AOCS supports three modes: 3-axis stabilized, spinning and tumbling. By superposition of a nutation angle, a motion of any grappling interface at the client surface of up to 4°/s can be obtained. For preparation of the capturing process the RvD payload of the servicer controls a commandable surface-to-surface distance to the client satellite in the range between 1 m and approx. 2.5 m within a spherical tolerance range of 7 cm.

Stereo images from the client taken by the servicer's RvD payload during an observation time of about 2 minutes (Fig. 1a) will be used by the Payload Control System software on ground to determine the client motion and to predict the movement profile. The images also serve for identification of the final grasping point.

Manipulator motion planner software running online in the PCS calculates the motion profile and prepares data for uplink to the robot in space for immediate execution.

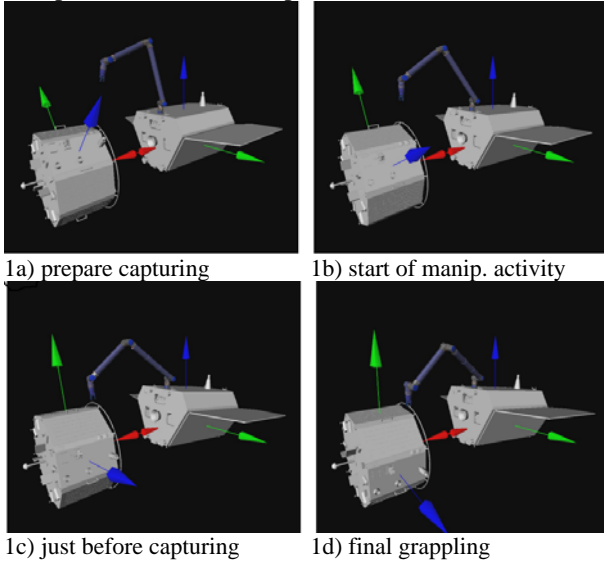


Figure 1: Capturing of the tumbling client

Small errors between the calculated and the true gripper position may occur. Therefore visual servoing is planned to be implemented which computes the relative position by analysing manipulator stereo camera data and delivers correction commands which additionally consider the actual robot joints position data.

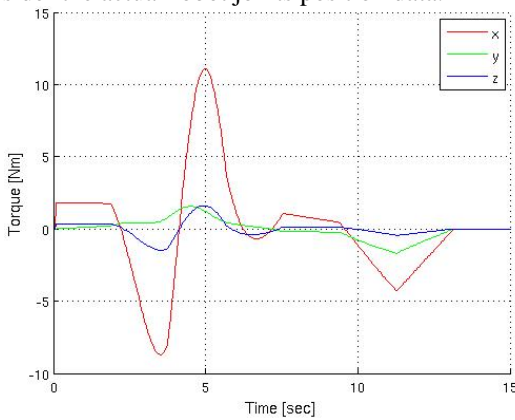


Figure 2: Torques on end-effector

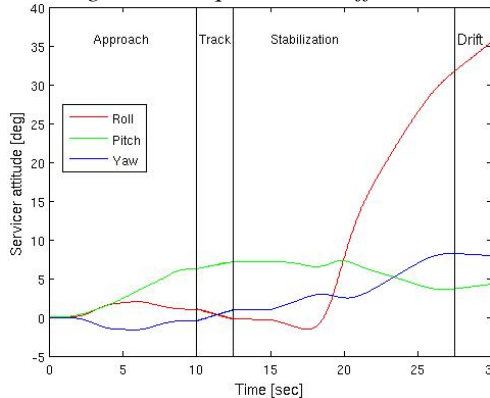


Figure 3: Servicer attitude after capturing

The loads on the end-effector during capturing and the servicer attitude during the stabilization phase before reactivation of its AOCS are depicted in Fig. 2 and Fig. 3, respectively. In the simulation it is assumed that both satellites' AOCS actuators are passive.

The capturing will be performed in a “supervised autonomy” mode where complementary on-board functions and on-ground functions are executed without ground operator interaction under normal conditions. Only in case of anomalies, unexpected behaviour, or if on-board FDIR reactions are not be initiated properly, the operator will take over control.



Figure 4: Robot arm for tele-presence control

In addition to the supervised autonomy mode, where the manipulator on board the servicer executes pre-determined motion profiles, the A&R payload also supports a tele-presence mode, where the manipulator motion and grappling in space is steered through ground operator guidance using a commercial robot arm as haptic input device. This tele-operation mode is a driver for absolutely minimum control loop latency.

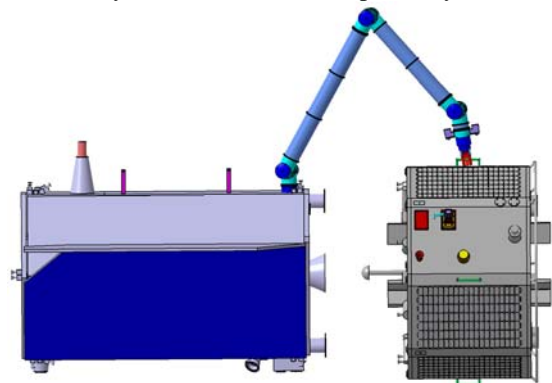


Figure 5: Berthing in progress

For final berthing and locking of the client satellite the manipulator guides the client with the penetrator pin into the berthing and docking mechanism on the servicer (see section 3.4). Fig. 5 illustrates the process. In order to grasp an uncooperative client satellite two major control strategies are possible for the spacecraft

carrying the robot: The spacecraft is allowed to move in reaction to the robot movements, while in the second case the AOCS intervenes to limit or eliminate any spacecraft motion (therefore the spacecraft can be kept stationary within the operational space). While the first case is more interesting for reducing fuel consumption for spacecraft control and is safer since jerky motion arising from thrusters is avoided, the second case is simpler to tele-operate and may be necessary for fulfilling spacecraft motion constraints (e.g. attitude motion may be limited for communication purposes).

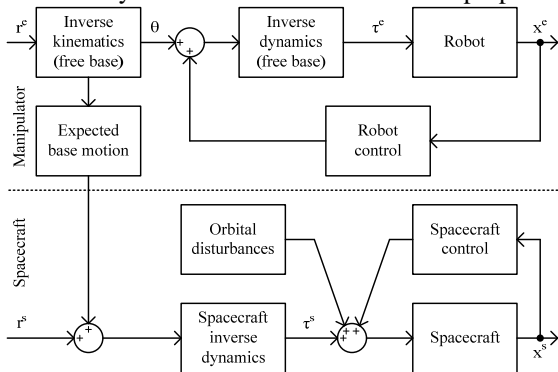


Figure 6: Control structure

Due to the fact that the AOCS cannot counteract the high dynamic disturbances stemming from the arm motion, for DEOS the platform will be treated as free floating. An input command is transformed by the kinematics of a free-floating robot into equivalent joint commands (see Fig. 6). The spacecraft control does not compensate for the robot motion, but also the spacecraft itself is no longer fixed in the operational space. The inverse kinematic solution provides the expected spacecraft motion, which is fed as a reference to the spacecraft controller. However, since the orbital disturbances are negligible within the duration of a single experiment, the whole spacecraft control block may be omitted, thus the AOCS actuators can be switched off completely.

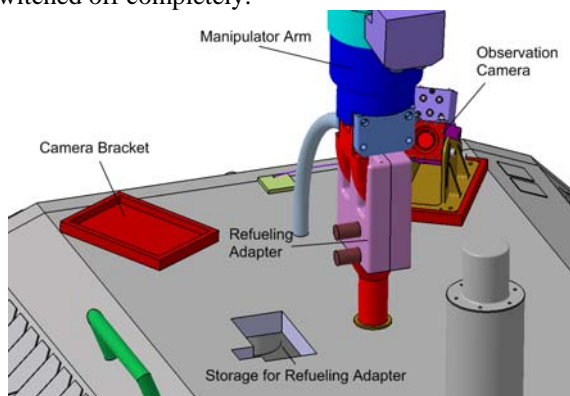


Figure 7: Gripper holding refuelling adapter

2.2. On-orbit servicing Demonstration

On-orbit servicing comprises two main tasks for the manipulator: relocation of an observation camera unit

from one bracket to a second one including activation of electronic connections and execution of a refuelling experiment. The on-orbit servicing experimental set-up on the client including the observation camera is illustrated in Fig. 7. The level of complexity of the refuelling experiment is still under investigation.

2.3. De-orbiting

For de-orbiting the manipulator holds the client satellite against the servicer with a client orientation such that client thrusters can decelerate the rigidly coupled pair for a controlled re-entry.

3. DEOS AUTOMATION AND ROBOTICS SERVICER PAYLOAD DESCRIPTION

3.1. Overview

The automation and robotics payload comprises a manipulator system with the manipulator arm, cold redundant stereo cameras and a target illumination system, a berthing and docking mechanism (BDM), and an Instrument Control Unit (ICU) which controls the A&R payload space segment and communicates with the On-Board Computer (OBC) of the Servicer.

3.2. DEOS Manipulator

Robotic Arm

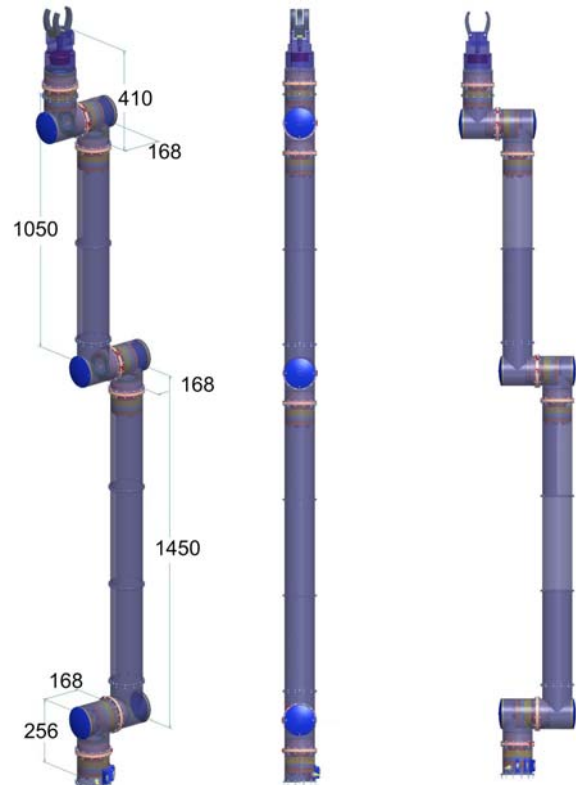


Figure 8: DEOS manipulator kinematics

The manipulator, equipped with a gripper and a stereo camera system mounted to the gripper, has to follow the residual movements of a selected object on the client

(e.g. structure part), grasp the part and finally eliminate the relative motion between both satellite bodies. Thus the manipulator has to be long enough to reach the grasp elements on the client and to damp the residual relative motion within its available operational working space. These top level requirements led to a manipulator design as shown in Fig. 8. The overall length of the 7 DoF arm, measured from base to the tip of the finger is 3232 mm. The manipulator system has a mass of 40.5 kg and a max power consumption of ~ 100 W during operation. When joint motors are inactive the power draw is 50 W only.

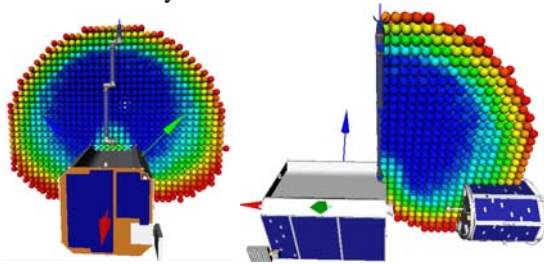


Figure 9: Manipulator reach

The following DEOS requirements apply:

- The arm kinematics has to provide max reach and dexterity in order to perform the capturing of the client independent from the client's main spinning axis.
- The arm shall be kinematically redundant to avoid joint-singularities during the capturing process
- The arm shall be stowable during launch within the given space on the servicer satellite.



Figure 10: ROKVISS joint

The reach of the DEOS manipulator is depicted in Fig. 9. Within the blue shaded area the number of possible gripper orientations is very high compared to the red shaded area at the border where only a few possible gripper orientations (rotation around the gripper's x-axis) exist.

The joint elements for the DEOS manipulator are based on the ROKVISS development (Fig. 10). The reliability of the ROKVISS joint elements was successfully proven by their operation in free space environment

from February 2005 until November 2010. They will be returned to Earth for a detailed investigation in 2011.

Despite the success, the DEOS requirements as well as some lessons learned from ROKVISS impose some modifications: electronics redundancy, new gear output position sensor and interconnecting joints bus interface (EtherCAT) and introduction of a new parking brake.

Manipulator Electronics and Sensors

For reliability reasons the electronics of each joint of the manipulator is designed as a cold redundant system. The joint electronics comprises a joint controller and a motor controller. The motor control unit will be realized with a motion control DSP. This high integrated "system on chip" combines all required peripheral units to drive a brushless DC motor with space vector modulation in combination with a high frequency current control loop. Of course, the motor phase current is supplied by motor power electronics with over current protection. The joint control algorithm runs on a floating point DSP which is coupled to all its necessary peripheral. Both processors are interconnected via a dual ported RAM. This minimizes the need of additional processor synchronization and enlarges the communication bandwidth between both units.

A motor position sensor (needed for motor commutation) and 3 phase current sensors (needed for current control) are connected to the motion control DSP. The 3 phase current sensors are located within the motor power electronics section.

The joint position sensor and the joint torque sensor are integrated on the drive side of the joint. They are connected to the joint control DSP enabling position-, torque- and impedance joint control. In addition to this, each joint contains several housekeeping sensors (e.g. temperature monitoring) and, of course, security sensors (e.g. over current protection and hardware end stop switches).

In case of a system malfunction the overall robot control unit is able to activate the redundant electronic path instead of the nominal path. Due to the fact that both paths are identical, no further settings have to be done. A special DLR-RM patented circuit guarantees that both motor power electronics could be tied to one motor winding. This is because a trade off has proven that a motor with redundant windings lead to more weight but not to more functional reliability. The new gear output position sensor is based on the magneto resistive effect.

The EtherCAT technology (www.ethercat.org) overcomes the system limitations of other Ethernet solutions, is still compatible with Ethernet and provides important advantages for a configuration with functional redundancy as shown in Fig. 11: in case of an interrupted communication line or a malfunctioning slave, the slave units behind cannot be addressed. A second Ethernet controller integrated into the ICU allows implementing an EtherCAT ring topology which will drastically increase the reliability of the entire

manipulator arm as shown in Fig. 12. The seven joint elements and the gripper will behave as slaves.

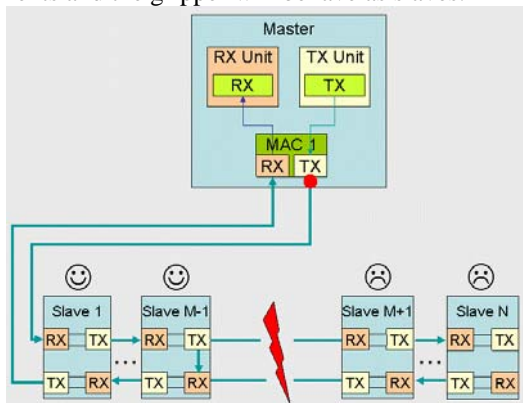


Figure 11: EtherCAT standard application

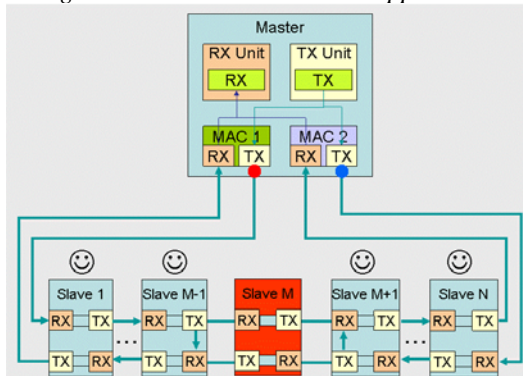


Figure 12: EtherCAT ring topology

Brakes

A DEOS requirement calls for parking brakes to be integrated into each joint which are engaged when the joint is not moving. A functional analysis showed that a brake mechanism acting on the gear input (between motor and harmonic drive) is the best suitable solution because it leads to a design with much lower volume and power requirements, compared to a solution with the brake at the gear output side: a brake block is pushed against the brake disk by means of a spring. A small electromagnetic drive mechanism will open and close the brake, when power is off, the brake is automatically closed.

Gripper

The purpose of the DEOS gripper is to capture a structure part at the moving client satellite and to handle objects during the planned on orbit servicing experiments. The torque, required to grasp and stabilize the DEOS client satellite, never exceeds 3 Nm and does therefore not present a design driver for the gripper, but the loads required to handle the objects of the manipulation experiments are relevant for the gripper design.

For the sake of modularity the gripper electronics is the same as for the manipulator joint elements and behaves similar to an additional joint from the communication point of view. The gripper is driven from an ILM 70

motor, as successfully used in ROKVISS. The motor-torque is applied via a spindle-gear to a toggle-lever mechanism which allows a very fast closing speed at the beginning and a very high grasp force at the end of the closing motion (see Fig. 13).

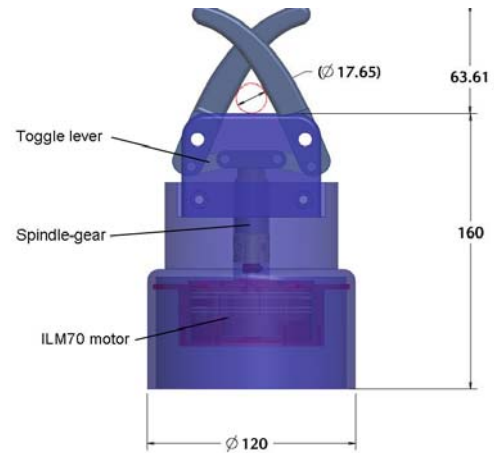


Figure 13: DEOS gripper

Joint Control Structure

The joint level controller is a joint state feedback controller with compensation of gravity and friction. The state vector contains the motor position, the joint torques, as well as their derivatives. By the appropriate parameterization of the feedback gains, the controller structure can be used to implement position, torque or impedance control. The gains of the controller can be computed in every Cartesian cycle, based on the desired joint stiffness and damping, as well as depending on the actual value of the inertia matrix. Hence, this controller structure provides active vibration damping of the flexible joint structure, maximizes the bandwidth of the joint control for the given instantaneous values of the inertia matrix, and implements variable joint stiffness and damping.

Three different strategies for implementing Cartesian compliant motion are realized: Admittance control, which accesses the joint position interface through the inverse kinematics; Impedance control, which is based on the joint torque interface; and Cartesian stiffness control, which accesses the joint impedance controller.

3.3. Manipulator Vision System

The manipulator vision system is the primary sensor during berthing and the on-orbit servicing experiments.

It is fully redundant and comprises a stereo camera with electronics and a laser-based illumination system. The stereo cameras have a field of view of $44.4^\circ \times 30.4^\circ$, a resolution of 384×256 pixels, a frame rate of up to 10Hz and a stereo base of approximately 5cm. Both sensors in one stereo camera are synchronized and they utilize the STAR1000 sensor, a radiation hard grayscale CCD device, which provides a sufficient SNR. Fig. 14 shows

the setup and view of the manipulator camera during capturing of the Client. The cameras are tilted around the horizontal axis, so that the gripper can be seen by the human operator.

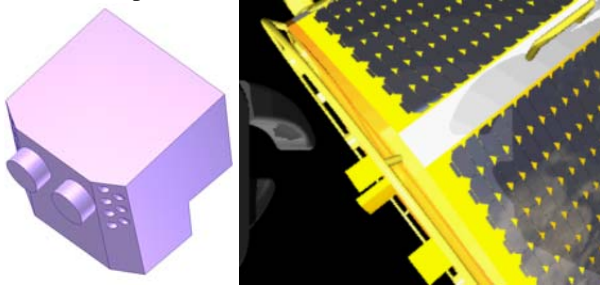


Figure 14: Setup and view of the manipulator camera

As the natural illumination conditions may not be sufficient, an additional artificial Target Illumination System (TIS) is foreseen. Several laser diodes are located in a sealed housing and a micro-lens array is used to illuminate the camera's field of view and to achieve a homogenous illumination. The TIS must be able to achieve sufficient irradiation of shadowed areas, so that areas exposed to direct sunlight and areas illuminated by the TIS can be seen by the camera without over- or underexposed spots. A radiometric analysis has shown that the irradiance of the TIS should be at least 10% of the sunlight. For the whole spectrum, this would require vast amounts of optical power. Thus, a filter with a small bandwidth of 20nm is used, which reduces the irradiance of the sun to 22.5 W/m². Due to the wavelength drift with temperature and operating current, the filter bandwidth cannot be reduced further. In addition, it is desirable to minimize the exposure time in total darkness. Thus, an optical power of 8W is sufficient to illuminate the whole field of view of the cameras at the working distance of up to 2m with an irradiance of 4.5W/m². In order to reduce the large thermal dissipation of laser diodes, the optical power of the target illumination system is adjustable and the laser diodes will be operated in a pulsed mode, where they are only active during the exposure time of the cameras. This is realized by synchronizing the laser diodes with the cameras and using a duty cycle of 100ms and pulse duration of 10ms to 20ms.

Another important sensor for manipulator control is the close-range camera of the RvD payload. The Close-Range Camera is a stereo camera with a stereo base of 12cm and has a field of view of 94.9° and acquires images with a resolution of 1024x1024 pixels at a frame rate of 1Hz. It covers the whole Client during berthing and is used to estimate the position, pose and motion of the client before the actual berthing is performed. Again, the images are transmitted to ground, where the image processing is performed by PCS software.

The images of both cameras, the manipulator and the close range camera, have to be transmitted to ground through a communication channel of 4Mbit / sec, already including other data such as satellite

housekeeping or haptic data. The net data rate for image data is approximately 3Mbit / sec. Up to four images with different frame rates and different resolutions have to be transmitted simultaneously. Consequently, the camera images have to be compressed before they are transmitted to ground. Two different methods are foreseen, a standard JPEG compression (e.g. for monitoring or telepresence) and a custom compression algorithm. Custom compression comprises an edge detection algorithm followed by a lossless compression of either the edge image or a sparse image. A compression rate of 5 to 20 has to be achieved. Pre-processing algorithms like noise reduction or rectification will be included before the image compression using a dedicated FPGA.

3.4. Berthing and Docking Subsystem

The Berthing and Docking Subsystem of the DEOS satellites is needed for the execution of docking, to lock the satellites together at the end of the berthing process and during the execution of the OOS demonstration program. It consists of the Berthing and Docking Mechanism (BDM), the Docking Camera attached to the lower end of the BDM and a light pattern at the Client's panel oriented to the Servicer satellite during docking. The Docking Camera as sensor system in combination with the light pattern provides relative position and angular misalignment information for the Servicer AOCS during final approach.

The BDM consists of two elements. The active docking part is located inside the Servicer satellite at the base plate, the passive docking part at the outside of the Client satellite base plate. The mechanism design bases upon a 'Snap' principle as outlined below. Three similar catch mechanisms are arranged over 120° around the docking cone. These catch mechanisms have two rotational degrees of freedom, one for the complete mechanism and a second one for the snap mechanism that is part of the catch mechanism. A compression-spring provides a force to keep or to bring back the snap mechanism into its resting position. A belt drive moves a worm gear via two spur gears, which rotate the catch mechanism. A nominal docking and undocking sequence without angular or position misalignment is shown in Fig. 15.

During final approach the BDM is in the approach position as shown in (1) in Fig. 15. As soon as the docking pin of the BDM passive part pushes the spring-loaded snap mechanism with sufficient force, the catch position (2) is entered. The Client's docking pin penetrates deep into the cone thereby pressing the snap mechanism and its spring in their respective end positions. This is only possible if the docking approach is performed with sufficient velocity and direction to overbear the spring force of the snap mechanism.

The Client is safely secured when the passive docking pin of the Client has passed the snap mechanism. To

finish the docking sequence the catch mechanism pulls the passive docking part to the end position inside the cone of the active part of the BDM into the latch position (4), pulling the Client to the Servicer satellite. In this position a pretension force caused by a spring at the base of the docking pin supports the fixation of the Client at the Servicer and the docking manoeuvre is completed.

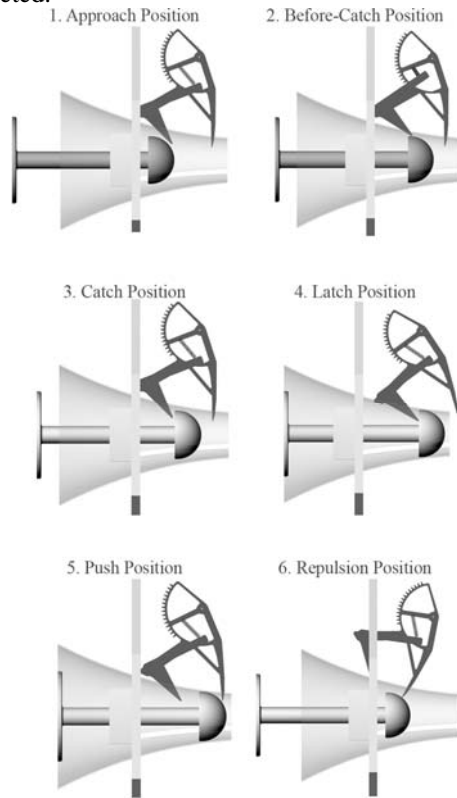


Figure 15: Docking and Undocking Sequence

Image (5) in Fig. 15 presents the push position that constitutes the starting point of the undocking sequence. The catch mechanism is slowly driven back. The catch mechanism, now acting as a pusher, makes contact with the hemisphere of the Client’s docking pin. In the following repulsion position (6) the catch mechanism is driven back so far, that the pusher can transfer sufficient impulse to the Client’s docking part that it leaves the Servicer’s BDM docking cone.

The viability of the design and feasibility of docking between Servicer and Client has been demonstrated by respective contact dynamic simulations not only for the nominal case but also for misaligned approach cases. For the multibody-simulation the Polygonal Contact Model (PCM) as described in [2] has been used for the cone of the BDM, the pin, the snap mechanism and the pushers that are part of the Client’s base plate. In the simulations performed so far, the angular and lateral misalignment between the satellite’s centre lines (cone and docking pin centre line) have been changed from 0° to $\pm 5^\circ$, and 0mm to 75mm, respectively.

The approach velocity of the Servicer satellite relative

to the Client is 0.01 m/s, for the simulations the two satellites are free floating (no active AOCS) at the moment of physical contact. The relative distance between Servicer and Client in all 3 axes for a nominal insertion profile (no angular misalignment) is shown in Fig. 16. Fig. 17 shows an example of the resulting contact forces at the cone-pin interface (active and passive part of the BDM).

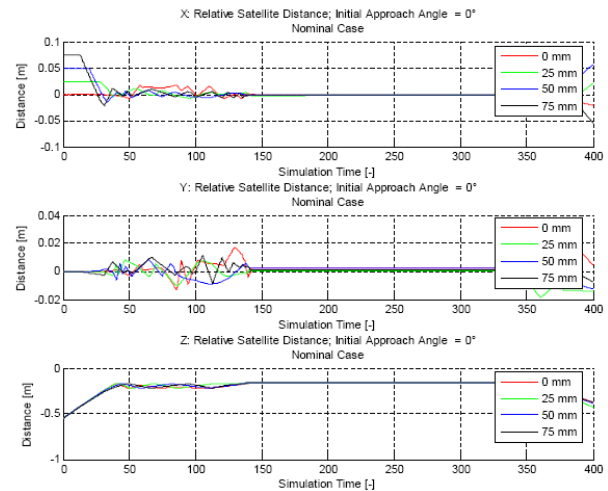


Figure 16: Relative distance between Servicer and Client during docking

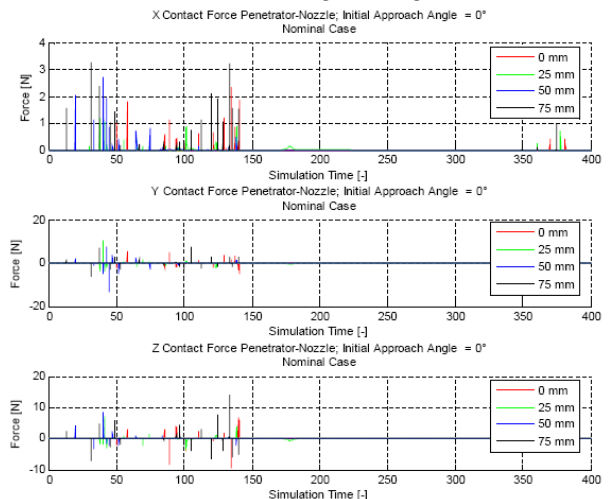


Figure 17: Results of contact dynamic simulations for docking without angular misalignment

The simulations consist of three phases: The approach and passing of the snap mechanism (0-100s), the latching (100-200s) and the undocking (200-400s).

At present the described Phase A design of the BDM is investigated for potential improvements reducing the complexity and single point failures by a single mechanism design instead of the three catch mechanisms arranged over 120° in the current concept.

3.5. Automation and Robotics ICU

The ICU comprises a master CPU board responsible for payload control and monitoring of all A&R payload

subsystems and for communication with the servicer OBC (status and housekeeping data for supervision, telemetry downlink uplink command reception and execution) and a slave CPU board with extremely high computing power 1100 MIPS (incl. margin) and floating point operation for control of the manipulator via EtherCAT @200 Hz per manipulator joint. A SpaceWire router is used for direct downlink of camera data via the servicer. Furthermore, a very low latency and jitter is allowed for the entire communication loop (haptic data downlink from the manipulator, routing and processing in the Ground Segment, and uplink from the ground computer to the manipulator via the ICU). The system uses the VxWorks operating system for MARCO (modular software framework for control of complex real-time systems developed by DLR-RM).

4. PAYLOAD CONTROL SYSTEM ON GROUND

The A&R Payload Control System (PCS) is part of the Flight Operations System in the Mission Control Centre (MCC), receiving telemetry frames (TM) and responding with telecommands (TC). The A&R PCS displays the relevant housekeeping data, controls the Berthing and Docking Mechanism and provides functions to set the parameters of the manipulator control, the manipulator vision system and the Berthing and Docking mechanism. Fig. 18 shows a schematic view of the A&R Payload Control System.

The Payload Operation Control Unit (POCU) is connected to a “Merger” of the Ground Data System of the MCC, unpacks the telemetry frames and distributes them to the other PCS sub-units. The images are uncompressed and displayed for monitoring in the Video Control Unit (VCU). The on-ground part of the manipulator control is conducted in the Manipulator Operation Control Unit (MOCU). Communication between the MOCU and the POCU and the POCU and the Manipulator Control on the satellite is performed with an update rate of 200Hz (256 kbps uplink) and a downlink data rate of 68.8kbit/sec.

During execution of the autonomous mode, the MOCU is controlled by the Image Processing Unit (IPU). It uses the uncompressed images as input for the actual image processing. During the observation phase, the IPU estimates the pose, position and motion of the client. This information is used by the MOCU to compute a trajectory. In the next step, the manipulator will execute this trajectory. During the execution, the IPU estimates the position and orientation of the handle on the client, which is used by the MOCU to update the trajectory in real-time. During execution of the tele-presence mode, a robot arm on ground (see Fig. 4) serves as a haptic input device, which is controlled by a human operator. Visual feedback is displayed to the operator by a three dimensional display or by a head-up display. By providing visual and haptic feedback, a high degree of immersion can be achieved allowing the operator direct

control of the manipulator on the Servicer.

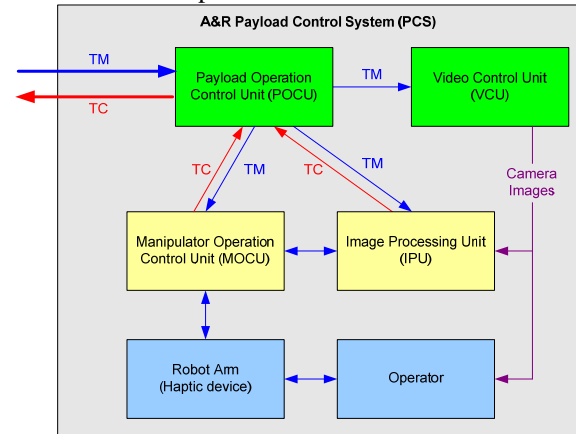


Figure 18: Schematic view of the A&R PCS

5. CONCLUSION

This paper presents the Automation and Robotics Payload on DEOS and its main tasks, the berthing of an uncooperative client and on-orbit servicing. The manipulator can either be operated supervised-autonomously or tele-operated by a human operator on ground. Furthermore, the paper gives an insight into the functionality of the major subsystems such as the manipulator arm, the berthing and docking mechanism and the vision system.

Challenges are the limited available computational power of radiation hardened CPUs on a satellite, the vision system including image processing, and complexity of handling non-nominal situations. Future work will include breadboarding of the manipulator arm and verification of the whole system in EPOS (European Proximity Operations Simulator), a robotic facility for pre-flight rendezvous and docking simulations.

6. REFERENCES

- [1] D. Reintsema, J. Thaeter, A. Rathke, W. Naumann, P. Rank, J. Sommer, DEOS – The German Robotics Approach to Secure and De-Orbit Malfunctioned Satellites from Low Earth Orbits, Robotics and Automation in Space (i-SAIRAS), 2010, Sapporo, Japan
- [2] Hippmann, G. (2003). An algorithm for compliant contact between complexly shaped surfaces in multibody dynamics. Multibody Dynamics 2003, Jorge A.C. Ambrosio (Ed.), IDMEC/IST, Lisbon, Portugal, July 1-4, 2003.

7. ACKNOWLEDGMENTS

The Phase B study for the DEOS Automation and Robotics payload is performed on behalf of the Space Agency of the German Aerospace Center DLR funded by the Federal Ministry of Economy and Technology (Förderkennzeichen 50 RA 0923).